JCTC Journal of Chemical Theory and Computation

Article

pubs.acs.org/JCTC

Reassessment of the Thermodynamic, Kinetic, and Spectroscopic Features of Cyanomethanimine Derivatives: A Full Anharmonic Perturbative Treatment

Fanny Vazart, Danilo Calderini, Dimitrios Skouteris, Camille Latouche, and Vincenzo Barone*

Scuola Normale Superiore, piazza dei Cavalieri 7, 56125 Pisa, Italy

Supporting Information

ABSTRACT: Herein we report a full thermodynamic and vibrational investigation of C-cyanomethanimine isomers rooted into the Density Functional Theory (DFT) and the second-order vibrational perturbation theory (VPT2). We show that an anharmonic treatment affects dramatically the vibrational behavior of the molecules, especially thanks to the inclusion of interaction terms between the various modes. Furthermore, the equilibrium constant between the isomers, as well as the rate constant, have been obtained at both harmonic and anharmonic levels showing, as expected, slight but non-negligible differences. To support our investigation, dispersion effects have been employed.

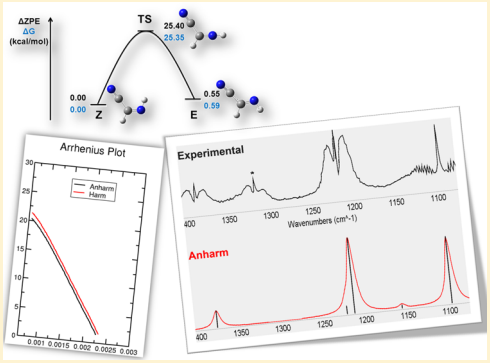

INTRODUCTION

Imines are able to undergo various transformations and act as reactive intermediates in a large panel of reactions of interest for health and biology in general.[1−4] Furthermore, over the past few years, the C═N moiety has attracted increasing attention,[5−8] also thanks to its putative role as intermediate in reactions involving purines and proteins.[9] Furthermore, the role of HCN in the interstellar space and prebiotic chemistry is also remarkable.[10−14]

Concerning astrochemistry and atmospheric studies, our group has been involved in investigations dealing with highly accurate vibrational spectra for both band positions and transition intensities.[15] It has been shown that only a very refined model, taking into account anharmonic effects, is able to retrace with accuracy the vibrational signatures of chemical compounds. Following our previous investigations on the thermodynamic and vibrational signatures of organic and inorganic molecules at the anharmonic level,[16−22] we present herein new insights based on the experimental and computed data obtained recently by Osman on the *Z*-C-cyanomethanimine (isomer *Z*) and *E*-C-cyanomethanimine (isomer *E*) molecules.[5] In previous papers, some of us highlighted the importance of modeling dispersion effects.[16,23] We investigated the vibrational and thermochemical properties of both molecules and the transition state connecting them (Figure 1), taking into account the most refined model available so far. We also report computations of the reaction rate at both harmonic and anharmonic levels. Comparisons with experimental data and harmonic level of theory are shown. All these results point out once again the non-negligible impact of anharmonicity on the chemical processes involving even small molecules.

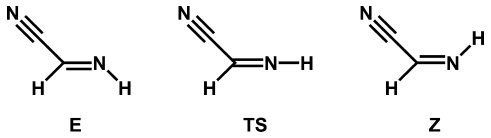

Figure 1. *E*-C-cyanomethanimine (*E*), Transition State (TS), and *Z*-C-cyanomethanimine (*Z*).

COMPUTATIONAL DETAILS

All calculations have been carried out with a development version of the Gaussian suite of programs.[24] Most of the computations were performed with the B3LYP hybrid density functional,[25−27] in conjunction with the SNSD basis set.[28] Additional computations have been performed with the double-hybrid B2PLYP functional[29] and with the second-order Møller−Plesset perturbative many body treatment (MP2),[30−34] in conjunction with the m-aug-cc-pVTZ basis set,[35,36] where *d* functions on hydrogens have been removed. Semiempirical dispersion contributions were also included into DFT computations by means of the D3 model of Grimme, leading to B3LYP-D3 and B2PLYP-D3 models.[37,38] Full geometry optimizations have been performed for both *Z* and *E* isomers checking the nature of the obtained structures by diagonalizing their Hessians. Cubic and semidiagonal quartic force constants have been next computed by finite differences

Received: December 18, 2014

DOI: 10.1021/ct501147a
J. Chem. Theory Comput. XXXX, XXX, XXX−XXX

of analytical Hessians and used to obtain anharmonic frequencies with the GVPT2 model taking into proper account possible resonances for frequencies[39] together with IR intensities with the DVPT2 model including both mechanical and electrical anharmonicities.[20,40]

At this level, the vibrational energy of asymmetric top molecules can be written

$$E_{\mathrm{vib}} = E_0 + \sum_i \frac{h}{2\pi}\omega_i n_i + \sum_{i\le j}\chi_{ij}\left(\frac{1}{2}n_i + \frac{1}{2}n_j + n_i n_j\right) \tag{1}$$

where E_0 is the zero-point energy, h is the Planck constant, and n_i and ω_i are the vibrational quantum numbers and harmonic wavenumbers, respectively; χ_{ij} is the anharmonic coupling between modes i,j, which is an explicit function of cubic and semidiagonal quartic force constants.[20,39,40] For transition states (TS), all the sums exclude the mode corresponding to the imaginary frequency. Those contributions enter in the semiclassical definition of reaction probability proposed by Miller,[41] which includes both tunneling and anharmonicity, and has been used in the present paper for the evaluation of reaction rates.

All the spectra have been generated and managed by the VMS-draw graphical user interface.[42]

The anharmonic CN stretching frequency was not in a satisfactory agreement in the case of B3LYP(+D3). This problem can be traced back to a bad description at the harmonic level because the Δ(Harm.-Anharm.) is almost identical for all levels of theory (ca. 30−40 cm^{-1}). To solve this issue, a Scale Factor (SF) on CN stretching has been set up on the HCN molecule and will only be applied on the harmonic CN frequency of both Z and E isomers, when needed. Then, the anharmonic correction is added to this new value. This SF is defined as below

$$\mathrm{SF} = \frac{\upsilon_{\mathrm{exp}} + \Delta(\nu_{\mathrm{Harm.}} - \nu_{\mathrm{Anharm.}})}{\nu_{\mathrm{Harm.}}} \tag{2}$$

with υ_{CN} = 2097 cm^{-1} (H−C≡N).[43] The values are reported in the Supporting Information.

Densities of States and Partition Functions. The principal quantities needed for thermodynamic and kinetic calculations are the partition functions (at different temperatures), which can be generally obtained from the microscopic density of states through a Boltzmann integral

$$Q(T) = \int_{\infty}^{0} \rho(E) \times e^{-((E-E_0)/(k_\beta T))}\mathrm{d}E \tag{3}$$

and the density of states $\rho(E)$ is calculated directly from the energy level structure. If the system is composed of N independent degrees of freedom, the overall partition function is given by the product of the individual partition functions, i.e. $Q(T) = Q_{\mathrm{tr}}(T) \times Q_{\mathrm{rot}}(T) \times Q_{\mathrm{vib}}(T)$. Dealing with isomerization reactions, the translational contribution $Q_{\mathrm{tr}}(T)$ is the same for all stationary points and can be neglected in the evaluation of equilibrium and rate constants. Next, for 3-dimensional rotations, the density of states is given by

$$\rho_{\mathrm{rot}}(E) = \frac{2}{\sigma}\sqrt{\frac{E}{ABC}} \tag{4}$$

where σ is the Rotational symmetry number, and A, B, and C, are the rotational constants. The challenging part is the computation of the vibrational density of states for an anharmonic system, both because of the nonconstant energy level spacing and because of the coupling of different vibrations (see eq 1). For the computation of the anharmonic vibrational density of states we have implemented a random walk Wang−Landau algorithm,[44−46] which scales very favorably with the dimension of the system.

Thermodynamic Functions. Through the partition functions and their temperature dependence we obtain the thermodynamic functions (enthalpy, entropy, and Gibbs free energy) of both isomers, according to

$$H = E_0 + k_\beta T + k_\beta T^2\left(\frac{\partial \ln Q}{\partial T}\right) \tag{5}$$

$$S = k_\beta T\left(\frac{\partial \ln Q}{\partial T}\right) + k_\beta \ln Q \tag{6}$$

$$G = H - TS = E_0 + k_\beta T(1 - \ln Q) \tag{7}$$

Equilibrium and Rate Constants. We have calculated both microcanonical (fixed E) and canonical (fixed T) equilibrium and rate constants. For the microcanonical ensemble (assuming the reaction is written as $E \Leftrightarrow Z$), the equilibrium constant is given by

$$K_{\mathrm{eq}}(E) = \frac{\rho_Z(E)}{\rho_E(E)} \tag{8}$$

where ρ_Z and ρ_E are, respectively, the densities of states of the two species at energy E. On the other hand, in the canonical ensemble, the equilibrium constant is given by

$$K_{\mathrm{eq}}(T) = \frac{Q_Z(T)}{Q_E(T)} \times e^{-((\Delta E)/(k_\beta T))} \tag{9}$$

where Q_Z and Q_E are, respectively, the partition functions of the two species, and $\Delta E = E_0(Z) - E_0(E)$ is the difference of their zero-point energies. As far as the corresponding rate constants are concerned, we will use the semiclassical transition state theory (SCST).[41] In this model, the microcanonical rate constant for the forward reaction is given by

$$k(E) = \frac{N(E)}{h\rho_E(E)} \tag{10}$$

where $N(E)$ is the sum of states for the transition state, corrected for the possibility of tunnelling and quantum reflection

$$N(E) = \sum_{n_1=0}\sum_{n_2=0}\cdots\sum_{n_{F-1}=0} P_n(E) \tag{11}$$

with the semiclassical tunneling probability given by

$$P_n(E) = \frac{1}{1 + e^{2\vartheta(n,E)}} \tag{12}$$

In the above equations, F-1 is the total number of vibrational degrees of freedom orthogonal to the reaction path. In the framework of VPT2, $\vartheta(n,E)$ is an explicit function of the harmonic and anharmonic force constants.[41] Using the Wang−Landau algorithm, it is possible to evaluate effectively $N(E)$ separating the energy range in small bins (with width δE)

DOI: 10.1021/ct501147a
J. Chem. Theory Comput. XXXX, XXX, XXX−XXX

Table 1. Experimental and Calculated Vibrational Wavenumbers (cm^{-1}) of *Z* and *E* Isomers

Z						*E*						
Osman[a]		B3LYP-D3/SNSD		B2PLYP-D3/m-aug		Osman		B3LYP-D3/SNSD		B2PLYP-D3/m-aug		
exp	calc	Harm.	Anharm. (with SF)	Harm.	Anharm.	exp[b]	calc[a]	Harm.	Anharm. (with SF)	Harm.	Anharm.	assignment[a]
3306	3334	3456	3286	3462	3295	3288	3456	3472	3302	3477	3310	ν_1 N−H str.
2943	3037	3128	2955	3161	2963	3050−2930	3076	3069	2906	3103	2931	ν_2 C−H str.
2239	2251	2332	2300 (*2225*)	2259	2220	2246	2336	2345	2312 (*2237*)	2275	2235	ν_3 C≡N str.
1599	1617	1672	1635 (*1582*)	1648	1609	1609	1678	1681	1644 (*1591*)	1663	1625	ν_4 C═N str.
1388	1362	1410	1377	1425	1391	1386	1402	1407	1370	1415	1379	ν_5 C−H bend
1218	1203	1243	1213	1248	1218	1218	1237	1239	1212	1242	1216	ν_6 CNH bend
904	922	917	904	922	909	908	912	909	898	914	903	ν_7 C−C str.
	617	619	612	617	610		620	620	613	621	614	ν_8 NCC bend
	213	231	230	232	232		242	244	243	244	243	ν_9 CCN bend
1095	1093	1124	1097	1138	1109		1106	1106	1079	1119	1091	ν_{10} C═N tor.
815	846	845	833	846	835	800	827	824	812	829	817	ν_{11} C−H O.P.
	324	332	326	333	328		322	328	323	329	325	ν_{12} CCN O.P.

[a]From ref 5, calculations performed at the B3LYP/aug-cc-pVDZ level. [b]From ref 47.

$$N(E) = \delta E \sum_{i=1}^{E/\delta E} \rho(E_i)\langle P(E_i)\rangle \tag{13}$$

where $\langle P(E_i)\rangle$ is the average tunneling probability for the different vibrational quantum number choices leading to $E \in [E_i-\delta E, E_i+\delta E]$.

The corresponding canonical expression for the rate constant is

$$K(T) = \frac{1}{h}\frac{\int_{-\infty}^{+\infty} N(E)e^{-(E/(k_\beta T))}\mathrm{d}E}{Q_{re}(T)} \tag{14}$$

where $Q_{re}(T)$ is the reactants partition function.

In accordance with the principle of detailed balance, both in the canonical and microcanonical ensemble, the equilibrium constant is given by the ratio of the two rate constants (direct and inverse).

RESULTS AND DISCUSSION

Infrared Investigations. Table 1 lists the experimental and computed vibrational wavenumbers of *Z* and *E* isomers. Our calculations were performed at the harmonic and anharmonic levels, using the B3LYP-D3 and B2PLYP-D3 models in conjunction with the SNSD and m-aug-cc-pVTZ basis sets. The results from calculations using other levels of theory are given in the Supporting Information (Tables S1 and S2). We start our discussion on *Z* isomer where, as one can see, our computed results are close to experiment. The C−H and N−H stretchings issuing from the VPT2 model are in much better agreement with experiment than the scaled harmonic values of ref 5. The same behavior is observed concerning vibrations below 1500 cm^{-1}. However, the C═N and C≡N stretches are not sufficiently well described in our model (B3LYP-D3/SNSD level). To solve this problem, a Scale Factor at the harmonic level has been set up (cf. Computational Details). Addition of VPT2 anharmonic corrections to those scaled harmonic values leads to vibrational wavenumbers in remarkable agreement with experiment. It is noteworthy that B2PLYPD3 results do not require any scaling.

A peak with a very low intensity was reported by Evans and co-workers around 3180 cm^{-1}, hypothetically assigned to $2\nu_{C=N}$.[47] Thanks to our computations we now confirm this hypothesis. Indeed, this weak band is clearly assigned as an overtone (2 quanta) of the fourth vibration mode (C═N stretching). Using the B2PLYP-D3/m-aug-cc-pvtz level of theory, this value is computed at ≈3200 cm^{-1} (*Z* isomer), which is in very good agreement with experiment.

According to the available experimental data on the *E* isomer, the agreement is also satisfactory.[47] Concerning the CN stretching, the same SF has been used (B3LYP-D3 computations) as before to obtain even more reliable results for these vibrations.

Moreover, for both isomers, a set of resonances appeared for the C−H stretching, coupled with a combination band involving υ_4 and υ_5. For the sake of consistency, we always took the lowest value of this resonance in our assignment. Finally, we also stress that the MAE using B2PLYP-D3 and the m-aug-cc-pVTZ basis set is good (≈11 cm^{-1}). This value is appreciable because the lowest energy modes could not be compared due to the lack of experimental data. We now compare the experimental Infrared spectrum (wavenumbers and intensities) of *Z*-C-cyanomethanimine to our computations (B3LYP-D3/SNSD) at both harmonic and anharmonic levels of theory with respect to experiment (Figures 2 and 3). One should notice that the harmonic spectrum fits quite nicely in the 1000−1500 cm^{-1} region. However, it turns out that experimental and harmonic spectra show a more pronounced disagreement above 1500 cm^{-1}. On the other hand, the anharmonic spectrum exhibits a remarkable accuracy with respect to experiment on the investigated region. Furthermore, one can see the presence of simulated small hills around 1700−2000 cm^{-1} which correspond to a set of overtones and combination bands. When zooming in the region 1070−1400 cm^{-1} on the experimental and anharmonic simulated spectra (Figure 3), it can be observed that all the information given by the experimental spectrum can be retrieved in the simulated one but for one peak around 1310 cm^{-1}. This peak, also present in the IR spectrum of *Z*-prop-2-ynylideneamine (structurally close to *Z*-C-cyanomethanimine), was not assigned.[5]

Let us now focus attention on the 1070−1400 cm^{-1} region. It turns out that not only the vibrational wavenumbers of the C═N torsion is particularly well reproduced in our computations (1097 vs 1095 cm^{-1}) but also its intensity. Indeed, the experimental intensity of the CNH bend (1218

DOI: 10.1021/ct501147a
J. Chem. Theory Comput. XXXX, XXX, XXX−XXX

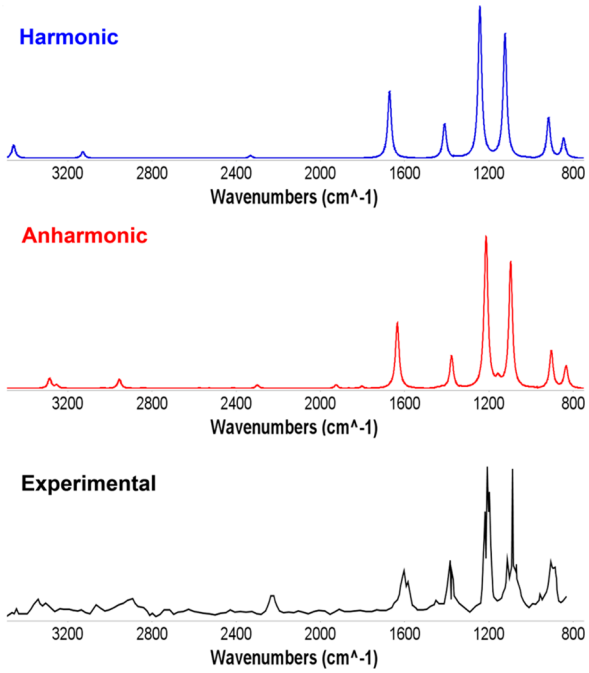

Figure 2. Observed (black, from ref 5) and simulated IR spectra of *Z*-C-cyanomethanimine (B3LYP-D3/SNSD): harmonic (blue) and anharmonic (red). Normalization has been performed with respect to the peak above 1200 cm^{-1}.

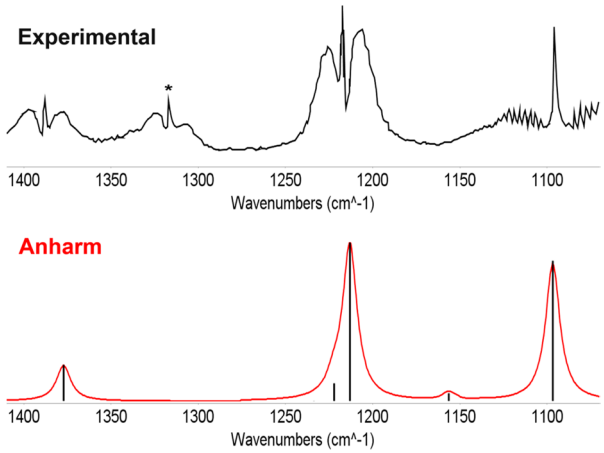

Figure 3. Observed FTIR (black, from ref 5) and simulated IR spectra of *Z*-cyanomethanimine (B3LYP-D3/SNSD) at the anharmonic (red) level in the region 1070−1400 cm^{-1}. Normalization has been performed with respect to the peak above 1200 cm^{-1}.

cm^{-1}) is considerably higher than that of the C═N torsion. This trend is also reproduced in our simulation and with a very accurate wavenumber (1213 cm^{-1}). Finally, the low intensity peak at 1388 cm^{-1} is also very well reproduced in our simulation.

Thermodynamics and Kinetics. The structures of *E* and *Z* isomers have been first optimized at several levels of theory. On those optimized geometries, analytical frequency calculations have been performed at the harmonic and anharmonic levels, the latter one by using the generalized second-order vibrational perturbation model.[48] In Table 2 are listed the energy differences (electronic energy (ΔE), zero-point corrected energy (ΔE_0), and Gibbs free energy (ΔG)) between both compounds at the harmonic level. The energy differences

Table 2. Energy Differences − Electronic Energy, Zero-Point Energy, and Free Gibbs Energy − between *E* and *Z* Isomers at the Harmonic Level (kcal/mol)

	SNSD	m-aug-cc-pVTZ	
Δ: (*E*)-(*Z*)	*B3LYP-D3*	*B2PLYP-D3*	*MP2*
ΔE	0.64	0.63	0.61
ΔE_0	0.54	0.54	0.54
ΔG	0.59	0.59	0.58

obtained without dispersion corrections and from anharmonic calculations are listed in the Supporting Information (Tables S3 and S4).

Table 2 shows a constant trend (the *Z* compound is always favored) and a negligible role of zero point and entropic effects. This result matches previous mixed computational and experimental investigations.[5,47] In order to understand the kinetics of the C-cyanomethanimine isomerization, the transition state between *Z* and *E* has been located and found ca. 25 kcal/mol higher than both stable isomers (Figure 4). This *TS* exhibits a linear C−N−H angle (≈180°) and sustains a substantial imaginary frequency (−1134 cm^{-1}).

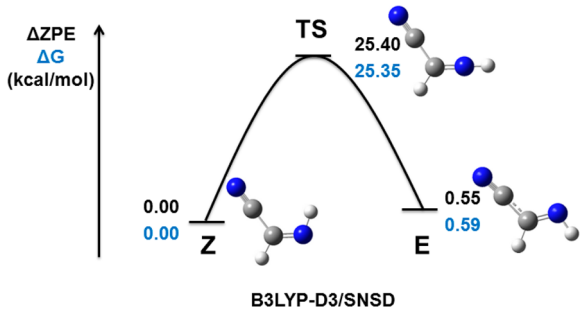

Figure 4. Relative energies (Zero-Point Energy -ZPE- and Gibbs Free Energy -Δ*G*-) diagram of the *Z*-C-cyanomethanimine⇔*E*-C-cyanomethanimine equilibrium calculated at the anharmonic B3LYP-D3/SNSD level (kcal/mol).

On these grounds a full kinetic investigation has been undertaken in order to compute the rate constant. We have computed the density of states of both isomers, as well as the transition state connecting them, by convolution of the 3D classical rotational DOS and the anharmonic vibrational DOS, obtained by the Wang−Landau algorithm. As sketched in the section devoted to Computational Details, the density of states permits a complete thermodynamic and kinetic characterization of the species. In particular, the enthalpy and entropy changes for the *Z*-to-*E* conversion are calculated as functions of temperature (Figures 5 and 6). In order to assess the effects of anharmonicity, these quantities are compared with the ones obtained using the harmonic vibrational density of states evaluated by the Stein-Rabinovitch modification of the Beyer−Swinehart algorithm.[49] The heat capacity at constant volume C_v (calculated from the slope of the enthalpy curve, after a trivial subtraction of a constant) is shown in the Supporting Information and has a convex profile that suggests a very modest variation up to temperatures around 2000 K. It must be stressed that, even though the Wang−Landau algorithm is valid for any energy interval, the quadratic approximation for vibrational energy levels issuing from the VPT2 model (see eq 1) loses reliability at high energies (corresponding to high temperatures) when the various dissociation limits of the

DOI: 10.1021/ct501147a
J. Chem. Theory Comput. XXXX, XXX, XXX−XXX

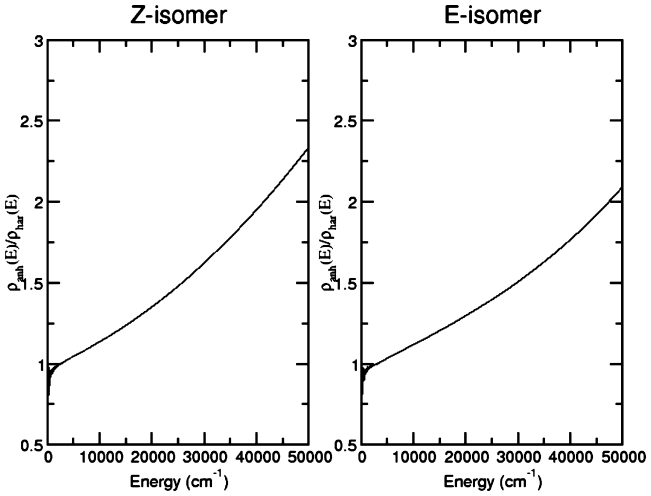

Figure 5. Evolution of the anharmonic factor, $F(E)$, for Z and E isomers.

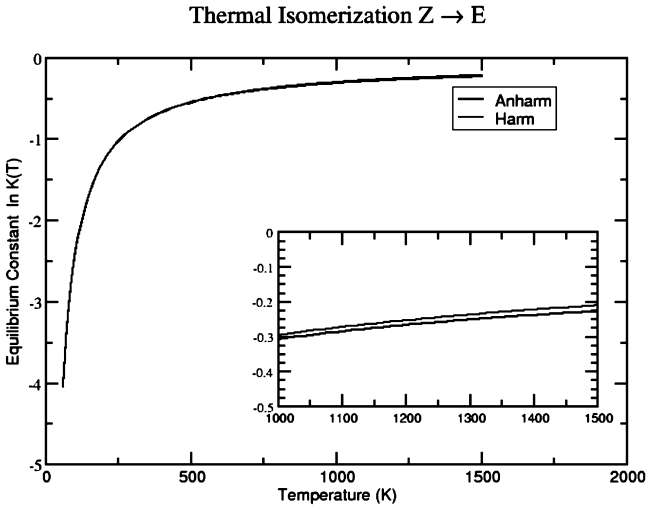

Figure 6. Ln of thermal equilibrium constant $K_{eq}(T)$ for the isomerization of cyanomethanimine.

vibrational modes are reached since, beyond the quadratic extremum, the energy tends to (unphysically) diminish with the quantum number. Consequently, as a reasonable compromise between reliability of the quadratic energy level formula and temperature range of the data reported, we have chosen a temperature of 1500 K as our upper limit. The trends of the two thermodynamic functions with temperature are very similar. This is to be expected, since the slope of the enthalpy change is the difference in heat capacities between products and reactants, whereas the slope of the entropy change is the ratio of the same quantity with temperature. In terms of absolute values, the reaction enthalpy is always positive. The main factor responsible for this is the higher zero-point energy of the E isomer. On the other hand, the entropy change is negative for the same reason, since fewer states are available to the E isomer. In the harmonic case, the enthalpy increases steadily and almost linearly with temperature, indicating an almost constant difference in heat capacities. This changes at very low temperatures, where the relative sparsity of E states diminishes its heat capacity and ultimately reverses the trend. Inclusion of anharmonicity has the effect of rendering the entropy change more negative, indicating that it increases the Z density of states more than the E one. Moreover, the difference in heat capacities between the two species becomes much more modest.

The effect of introducing anharmonicity in the density of states can be better evidenced in terms of the so-called anharmonic factor,[50] defined as the ratio of the corresponding densities of states

$$F(E) = \frac{\rho_{\mathrm{Anharm}}(E)}{\rho_{\mathrm{Harm}}(E)} \tag{15}$$

As shown in Figure 5, the anharmonic factor varies almost linearly with the energy. A similar trend was found by Troe et al.,[50] who compared harmonic and anharmonic densities of states for various small molecules. The high-frequency deviation in the low-energy region is related to the statistical sampling of the Wang−Landau algorithm.

It can be seen that the slope in the case of the Z-isomer is higher, indicating that anharmonicity increases the density of states more for the Z isomer than for its E counterpart. This trend is in agreement with the enthalpy and entropy curves shown above. Figure 6 shows the Ln of the equilibrium constant for the $Z \rightarrow E$ isomerization. At all temperatures considered, the equilibrium constant is less than one, and this effect is more pronounced at low temperatures where the enthalpy term dominates. As the temperature increases, the difference in zero point energies becomes increasingly less important, and the equilibrium constant approaches unity. Introducing anharmonicity lowers slightly the equilibrium constant. This appears principally to be an entropy effect since, as shown before, the entropy of the Z isomer is substantially larger than that of E, while the enthalpy contributions are very close.

Figure 7 shows the microcanonical and canonical rate constants for the direct reaction. Tunnelling and nonclassical

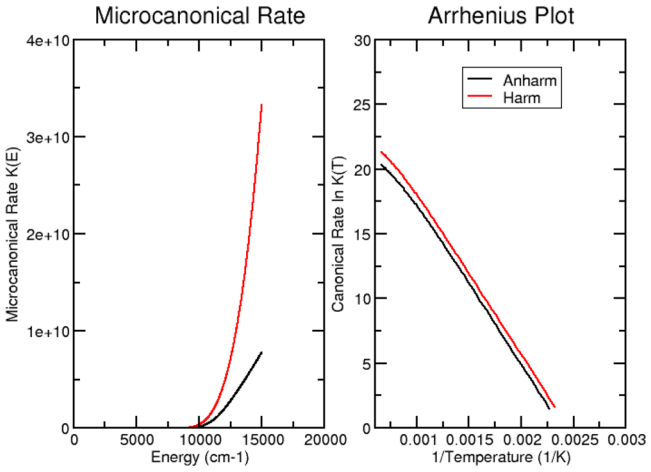

Figure 7. Microcanonical and canonical rate constants for the isomerization of C-cyanomethanimine.

reflection near the transition state have been included using the semiclassical approach of Miller and co-workers (even though, in this case, quantum effects are not expected to play any significant role, since the imaginary frequency of the transition state is only of the order of 1100 cm^{-1}).[41]

It can be seen that the anharmonic rates are lower than the harmonic ones at all energies and temperatures considered. It has already been shown how anharmonicity lowers the Gibbs

DOI: 10.1021/ct501147a
J. Chem. Theory Comput. XXXX, XXX, XXX−XXX

free energy of the reactants. This effect more than compensates the corresponding effect on the transition state, thus reducing the rate constant. From the Arrhenius plot, it is seen that the slope of the curve is essentially the same both in the harmonic and anharmonic case. Thus, the activation energy remains invariant on introduction of anharmonicity, which seems primarily to decrease the pre-exponential factor. The activation energy calculated from the slope of the Arrhenius plot is 23.9 kcal/mol, which is in nice agreement with the potential barrier of the system (25.4 kcal/mol).

CONCLUSION

In this paper, we have provided new insights concerning the behavior of C-cyanomethanimine. The infrared spectrum of *Z*-C-cyanomethanimine has been simulated, and the anharmonic spectrum matches nicely the experimental one. Furthermore, vibrational energies of *E*-C-cyanomethanimine have been also assigned. We have provided a complete thermodynamic characterization, leading to the computation of equilibrium constant between *Z* and *E*. Moreover the kinetics of the $Z \rightarrow E$ isomerization has been explored, and the effect of anharmonicity on the rate constant has been assessed. The reliability and effectiveness of the proposed computational protocol and its ongoing implementation in a widely available computer code pave the route for systematic investigations of more complex systems.

ASSOCIATED CONTENT

Supporting Information

Optimized geometries of *Z*, TS, and *E* at the B3LYP-D3/SNSD level of theory in Eckhart Orientation. Tables containing energies and vibrations for both isomers. This material is available free of charge via the Internet at http://pubs.acs.org.

AUTHOR INFORMATION

Corresponding Author

*E-mail: vincenzo.barone@sns.it.

Notes

The authors declare no competing financial interest.

ACKNOWLEDGMENTS

The research leading to these results has received funding from the European Union's Seventh Framework Programme (FP7/2007-2013) under grant agreement No. ERC-2012-AdG-320951-DREAMS. The authors gratefully thank the high-performance computer facilities of the DREAMS center (http://dreamshpc.sns.it) for providing computer resources. The support of the COST CMTS-Action CM1002 "COnvergent Distributed Environment for Computational Spectroscopy (CODECS)" is also acknowledged.

REFERENCES

(1) Adrio, J.; Carretero, J. C. Novel Dipolarophiles and Dipoles in the Metal-Catalyzed Enantioselective 1,3-Dipolar Cycloaddition of Azomethine Ylides. *Chem. Commun.* **2011**, *47*, 6784−6794.

(2) Erkkilä, A.; Majander, I.; Pihko, P. M. Iminium Catalysis. *Chem. Rev.* **2007**, *107*, 5416−5470.

(3) Ma, J.-A. Catalytic Asymmetric Synthesis of [small Alpha]- and [small Beta]-Amino Phosphonic Acid Derivatives. *Chem. Soc. Rev.* **2006**, *35*, 630−636.

(4) Nielsen, M.; Worgull, D.; Zweifel, T.; Gschwend, B.; Bertelsen, S.; Jorgensen, K. A. Mechanisms in Aminocatalysis. *Chem. Commun.* **2011**, *47*, 632−649.

(5) Osman, O. I. Experimental and Theoretical Investigation of the Pyrolysis Products of Iminodiacetonitrile, $(N{\equiv}CCH_2)_2NH$. *J. Phys. Chem. A* **2014**, *118*, 10934−10943.

(6) Morin, M. S. T.; Lu, Y.; Black, D. A.; Arndtsen, B. A. Copper-Catalyzed Petasis-Type Reaction: A General Route to A-Substituted Amides From Imines, Acid Chlorides, and Organoboron Reagents. *J. Org. Chem.* **2012**, *77*, 2013−2017.

(7) Zhang, E.; Tian, H.; Xu, S.; Yu, X.; Xu, Q. Iron-Catalyzed Direct Synthesis of Imines from Amines or Alcohols and Amines via Aerobic Oxidative Reactions under Air. *Org. Lett.* **2013**, *15*, 2704−2707.

(8) Morin, M. S. T.; St-Cyr, D. J.; Arndtsen, B. A.; Krenske, E. H.; Houk, K. N. Modular Mesoionics: Understanding and Controlling Regioselectivity in 1,3-Dipolar Cycloadditions of Münchnone Derivatives. *J. Am. Chem. Soc.* **2013**, *135*, 17349−17358.

(9) Ferris, J. P.; Hagan, W. J., Jr. HCN and Chemical Evolution: The Possible Role of Cyano Compounds in Prebiotic Synthesis. *Tetrahedron* **1984**, *40*, 1093−1120.

(10) Snyder, L. E.; Buhl, D. Observations of Radio Emission from Interstellar Hydrogen Cyanide. *Astrophys. J.* **1971**, *163*, L47.

(11) Balucani, N. Elementary Reactions and Their Role in Gas-Phase Prebiotic Chemistry. *Int. J. Mol. Sci.* **2009**, *10*, 2304−2335.

(12) Balucani, N. Elementary Reactions of N Atoms with Hydrocarbons: First Steps towards the Formation of Prebiotic N-Containing Molecules in Planetary Atmospheres. *Chem. Soc. Rev.* **2012**, *41*, 5473−5483.

(13) Balucani, N.; Bergeat, A.; Cartechini, L.; Volpi, G. G.; Casavecchia, P.; Skouteris, D.; Rosi, M. Combined Crossed Molecular Beam and Theoretical Studies of the N(2D) + CH_4 Reaction and Implications for Atmospheric Models of Titan. *J. Phys. Chem. A* **2009**, *113*, 11138−11152.

(14) Balucani, N.; Leonori, F.; Petrucci, R.; Stazi, M.; Skouteris, D.; Rosi, M.; Casavecchia, P. Formation of Nitriles and Imines in the Atmosphere of Titan: Combined Crossed-Beam and Theoretical Studies on the Reaction Dynamics of Excited Nitrogen Atoms N(2D) with Ethane. *Faraday Discuss.* **2010**, *147*, 189−216.

(15) Puzzarini, C.; Biczysko, M.; Bloino, J.; Barone, V. Accurate Spectroscopic Characterization of Oxirane: A Valuable Route To Its Identification In Titan's Atmosphere And The Assignment Of Unidentified Infrared Bands. *Astrophys. J.* **2014**, *785*, 107.

(16) Latouche, C.; Barone, V. Computational Chemistry Meets Experiments for Explaining the Behavior of Bibenzyl: A Thermochemical and Spectroscopic (IR, Raman and NMR) Investigation. *J. Chem. Theory Comput.* **2014**, *10*, 5586−5592.

(17) Baiardi, A.; Latouche, C.; Bloino, J.; Barone, V. Accurate yet Feasible Computations of Resonance Raman Spectra for Metal Complexes in Solution: $[Ru(bpy)_3]^{(2+)}$ as a Case Study. *Dalton Trans.* **2014**, *43*, 17610−17614.

(18) Latouche, C.; Palazzetti, F.; Skouteris, D.; Barone, V. High Accuracy Vibrational Computations for Transition Metal Complexes Including Anharmonic Corrections: Ferrocene, Ruthenocene and Osmocene as Test Cases. *J. Chem. Theory Comput.* **2014**, *10*, 4565−4573.

(19) Biczysko, M.; Panek, P.; Scalmani, G.; Bloino, J.; Barone, V. Harmonic and Anharmonic Vibrational Frequency Calculations with the Double-Hybrid B2PLYP Method. *J. Chem. Theory Comput.* **2010**, *6*, 2115−2125.

(20) Bloino, J.; Biczysko, M.; Barone, V. General Perturbative Approach for Spectroscopy, Thermodynamics, and Kinetics: Methodological Background and Benchmark Studies. *J. Chem. Theory Comput.* **2012**, *8*, 1015−1036.

(21) Carnimeo, I.; Puzzarini, C.; Tasinato, N.; Stoppa, P.; Charmet, A. P.; Biczysko, M.; Cappelli, C.; Barone, V. Anharmonic Theoretical Simulations of Infrared Spectra of Halogenated Organic Compounds. *J. Chem. Phys.* **2013**, *139*, 074310.

(22) Puzzarini, C.; Biczysko, M.; Barone, V. Accurate Harmonic/Anharmonic Vibrational Frequencies for Open-Shell Systems: Performances of the B3LYP/N07D Model for Semirigid Free Radicals Benchmarked by CCSD(T) Computations. *J. Chem. Theory Comput.* **2010**, *6*, 828−838.

DOI: 10.1021/ct501147a
J. Chem. Theory Comput. XXXX, XXX, XXX−XXX

(23) Fornaro, T.; Biczysko, M.; Monti, S.; Barone, V. Dispersion Corrected DFT Approaches for Anharmonic Vibrational Frequency Calculations: Nucleobases and Their Dimers. *Phys. Chem. Chem. Phys.* **2014**, *16*, 10112−10128.
(24) Frisch, M. J.; Trucks, G. W.; Schlegel, H. B.; Scuseria, G. E.; Robb, M. A.; Cheeseman, J. R.; Scalmani, G.; Barone, V.; Mennucci, B.; Petersson, G. A.; Nakatsuji, H.; Caricato, M.; Li, X.; Hratchian, H. R.; Izmaylov, A. F.; Bloino, J.; Zheng, G.; Sonnenberg, J. L.; Hada, M.; Ehara, M.; Toyota, K.; Fukuda, R.; Hasegawa, J.; Ishida, M.; Nakajima, T.; Honda, Y.; Kitao, O.; Nakai, H.; Vreven, T.; Montgomery, J. A., Jr.; Peralta, J. R.; Ogliaro, F.; Bearpark, M.; Heyd, J. J.; Brothers, E.; Kudin, K. N.; Staroverov, V. N.; Kobayashi, R.; Normand, J.; Raghavachari, K.; Rendell, A.; Burant, J. C.; Iyengar, S. S.; Tomasi, J.; Cossi, M.; Rega, N.; Millam, J. M.; Klene, M.; Knox, J. E.; Cross, J. B.; Bakken, V.; Adamo, C.; Jaramillo, J.; Gomperts, R.; Stratmann, R. E.; Yazyev, O.; Austin, A. J.; Cammi, R.; Pomelli, C.; Ochterski, J. W.; Martin, R. L.; Morokuma, K.; Zakrzewski, V. G.; Voth, G. A.; Salvador, P.; Dannenberg, J. J.; Dapprich, S.; Daniels, A. D.; Farkas, O.; Foresman, J. B.; Ortiz, J. V; Cioslowski, J.; Fox, D. J. *GDVH37p*; 2014.
(25) Stephens, P. J.; Devlin, F. J.; Chabalowski, C. F.; Frisch, M. J. Ab Initio Calculation of Vibrational Absorption and Circular Dichroism Spectra Using Density Functional Force Fields. *J. Phys. Chem.* **1994**, *98*, 11623−11627.
(26) Lee, C.; Yang, W.; Parr, R. G. Development of the Colle-Salvetti Correlation-Energy Formula into a Functional of the Electron Density. *Phys. Rev. B* **1988**, *37*, 785−789.
(27) Becke, A. D. Density-Functional Thermochemistry. III. The Role of Exact Exchange. *J. Chem. Phys.* **1993**, *98*, 5648−5652.
(28) SNSD, basis sets. 2013. http://compchem.sns.it/sites/default/files/download/gaussian/basis_sets/SNSD.gbs (accessed Jan 20, 2015).
(29) Grimme, S. Semiempirical Hybrid Density Functional with Perturbative Second-Order Correlation. *J. Chem. Phys.* **2006**, *124*, 034108.
(30) Frisch, M. J.; Head-Gordon, M.; Pople, J. A. A Direct MP2 Gradient Method. *Chem. Phys. Lett.* **1990**, *166*, 275−280.
(31) Frisch, M. J.; Head-Gordon, M.; Pople, J. A. Semi-Direct Algorithms for the MP2 Energy and Gradient. *Chem. Phys. Lett.* **1990**, *166*, 281−289.
(32) Head-Gordon, M.; Head-Gordon, T. Analytic MP2 Frequencies without Fifth-Order Storage. Theory and Application to Bifurcated Hydrogen Bonds in the Water Hexamer. *Chem. Phys. Lett.* **1994**, *220*, 122−128.
(33) Head-Gordon, M.; Pople, J. A.; Frisch, M. J. MP2 Energy Evaluation by Direct Methods. *Chem. Phys. Lett.* **1988**, *153*, 503−506.
(34) Sæbø, S.; Almlöf, J. Avoiding the Integral Storage Bottleneck in LCAO Calculations of Electron Correlation. *Chem. Phys. Lett.* **1989**, *154*, 83−89.
(35) Papajak, E.; Leverentz, H. R.; Zheng, J.; Truhlar, D. G. Efficient Diffuse Basis Sets: Cc-pVxZ+ and Maug-Cc-pVxZ. *J. Chem. Theory Comput.* **2009**, *5*, 1197−1202.
(36) Dunning, T. H. Gaussian Basis Sets for Use in Correlated Molecular Calculations. I. The Atoms Boron through Neon and Hydrogen. *J. Chem. Phys.* **1989**, *90*, 1007.
(37) Grimme, S.; Antony, J.; Ehrlich, S.; Krieg, H. A Consistent and Accurate Ab Initio Parametrization of Density Functional Dispersion Correction (DFT-D) for the 94 Elements H-Pu. *J. Chem. Phys.* **2010**, *132*, 154104.
(38) Goerigk, L.; Grimme, S. Efficient and Accurate Double-Hybrid-Meta-GGA Density Functionals—Evaluation with the Extended GMTKN30 Database for General Main Group Thermochemistry, Kinetics, and Noncovalent Interactions. *J. Chem. Theory Comput.* **2011**, *7*, 291−309.
(39) Barone, V. Anharmonic Vibrational Properties by a Fully Automated Second-Order Perturbative Approach. *J. Chem. Phys.* **2005**, *122*, 14108.
(40) Barone, V.; Biczysko, M.; Bloino, J. Fully Anharmonic IR and Raman Spectra of Medium-Size Molecular Systems: Accuracy and Interpretation. *Phys. Chem. Chem. Phys.* **2014**, *16*, 1759−1787.
(41) Miller, W. H.; Hernandez, R.; Handy, N. C.; Jayatilaka, D.; Willetts, A. Ab Initio Calculation of Anharmonic Constants for a Transition State, with Application to Semiclassical Transition State Tunneling Probabilities. *Chem. Phys. Lett.* **1990**, *172*, 62−68.
(42) Licari, D.; Baiardi, A.; Biczysko, M.; Egidi, F.; Latouche, C.; Barone, V. Implementation of a Graphical User Interface for the Virtual Multifrequency Spectrometer: The VMS-Draw Tool. *J. Comput. Chem.* **2014**, DOI: 10.1002/jcc.23785.
(43) CN stretching from HCN. http://webbook.nist.gov/cgi/cbook.cgi?ID=C74908&Mask=800#Electronic-Spec (accessed December 12, 2014).
(44) Wang, F.; Landau, D. Efficient, Multiple-Range Random Walk Algorithm to Calculate the Density of States. *Phys. Rev. Lett.* **2001**, *86*, 2050−2053.
(45) Basire, M.; Parneix, P.; Calvo, F. Quantum Anharmonic Densities of States Using the Wang-Landau Method. *J. Chem. Phys.* **2008**, *129*, 081101.
(46) Nguyen, T. L.; Barker, J. R. Sums and Densities of Fully Coupled Anharmonic Vibrational States: A Comparison of Three Practical Methods. *J. Phys. Chem. A* **2010**, *114*, 3718−3730.
(47) Evans, R. A.; Lorencak, P.; Ha, T. K.; Wentrup, C. HCN Dimers: Iminoacetonitrile and N-Cyanomethanimine. *J. Am. Chem. Soc.* **1991**, *113*, 7261−7276.
(48) Bloino, J.; Barone, V. A Second-Order Perturbation Theory Route to Vibrational Averages and Transition Properties of Molecules: General Formulation and Application to Infrared and Vibrational Circular Dichroism Spectroscopies. *J. Chem. Phys.* **2012**, *136*, 124108.
(49) Stein, S. E.; Rabinovitch, B. S. Accurate Evaluation of Internal Energy Level Sums and Densities Including Anharmonic Oscillators and Hindered Rotors. *J. Chem. Phys.* **1973**, *58*.
(50) Troe, J.; Ushakov, V. G. Anharmonic Rovibrational Numbers and Densities of States for HO_2, H_2CO, and H_2O_2. *J. Phys. Chem. A* **2009**, *113*, 3940−3945.

DOI: 10.1021/ct501147a
J. Chem. Theory Comput. XXXX, XXX, XXX−XXX